Biofabrication

International Society for Biofabrication

PAPER

Vascularized adipocyte organoid model using isolated human microvessel fragments

To cite this article: Hannah A Strobel *et al* 2021 *Biofabrication* **13** 035022

IOP Publishing Biofabrication 13 (2021) 035022 https://doi.org/10.1088/1758-5090/abe187

Biofabrication

PAPER

Vascularized adipocyte organoid model using isolated human microvessel fragments

Hannah A Strobel, Thomas Gerton and James B Hoying

Advanced Solutions Life Sciences, 500 N Commercial St, Manchester, NH 03101, United States of America

E-mail: jhoying@advancedsolutions.com

RECEIVED
20 November 2020

REVISED
22 January 2021

ACCEPTED FOR PUBLICATION
29 January 2021

PUBLISHED
7 April 2021

Keywords: organoid, vascularize, mesenchymal stem cell, adipose, microvessel

Supplementary material for this article is available online

Abstract

Tissue organoids are proving valuable for modeling tissue health and disease in a variety of applications. This is due, in part, to the dynamic cell–cell interactions fostered within the 3D tissue-like space. To this end, the more that organoids recapitulate the different cell–cell interactions found in native tissue, such as that between parenchyma and the microvasculature, the better the fidelity of the model. The microvasculature, which is comprised of a spectrum of cell types, provides not only perfusion in its support of tissue health, but also important cellular interactions and biochemical dynamics important in tissue phenotype and function. Here, we incorporate whole, intact human microvessel fragments isolated from adipose tissue into organoids to form both mesenchymal stem cell (MSC) and adipocyte vascularized organoids. Isolated microvessels retain their native structure and cell composition, providing a more complete representation of the microvasculature within the organoids. Microvessels expanded via sprouting angiogenesis within organoids comprised of either MSCs or MSC-derived adipocytes grew out of the organoids when placed in a 3D collagen matrix. In MSC organoids, a ratio of 50 MSCs to 1 microvessel fragment created the optimal vascularization response. We developed a new differentiation protocol that enabled the differentiation of MSCs into adipocytes while simultaneously promoting microvessel angiogenesis. The adipocyte organoids contained vascular networks, were responsive in a lipolysis assay, and expressed the functional adipocyte markers adiponectin and peroxisome proliferator-activated receptor gamma. The presence of microvessels promoted insulin receptor expression by adipocytes and modified interleukin-6 secretion following a tumor necrosis factor alpha challenge. Overall, we demonstrate a robust method for vascularizing high cell-density organoids with potential implications for other tissues as well.

1. Introduction

Tissue organoids are being used to study cellular behavior, interrogate tissue biology dynamics, and develop new pharmaceuticals [1, 2]. In some cases, organoids may also serve as building blocks for larger engineered tissues to be implanted [3]. As the utility of organoids expands, the composition of and approaches to building organoids has also progressed. Importantly, the inclusion of vascular cells, typically endothelial cells (ECs), into the organoid is seen as necessary to recapitulate more of the relevant native tissue biology, and potentially as a precursor to engraftment and perfusion. In addition to ECs, other cell types, such as smooth muscle cells, macrophages, stem cells, pericytes, and other immune cells can comprise and/or associate with the microvessel wall, and coordinate with ECs to influence angiogenesis, network formation, and vascular function [4–11]. These vascular cells also interact with other cellular components within the tissue to establish homeostasis, function, and, when dysregulated, disease.

Efforts to vascularize organoids *in vitro* have primarily focused on incorporating ECs as precursors to forming vessel segments [12–15]. In these cases, ECs self-assembled into a small number of capillary-like structures within organoids. While capturing some aspects of the vasculature, these single-EC type structures lack the structural and cellular complexity of the native microvasculature. Reflecting this, more

complex vascular elements within organoids have been produced by incorporating multiple microvascular cell types derived from induced pluripotent stem cells [16]. This, however, required lengthy, complicated, differentiation procedures [16]. There is still a strong need for an organoid vascularization solution that is robust, simple to implement, and translatable to multiple tissue systems.

Isolated microvessel fragments harvested from adipose tissue have proven effective at deriving new microvasculatures in a variety of applications. Microvessels are derived from all three general microvascular compartments (i.e. arterioles, venules, and capillaries), retain their intact native structure (including lumen) and cellular composition, and readily recapitulate angiogenesis and tissue vascularization when placed in 3D environments [17–22]. This is true for microvessels derived from mouse, rat, and human [19]. Importantly, as neovessels sprout and grow from the parent microvessels, they locate and inosculate with each other creating a network of neovessels that fills the tissue space [23]. Additionally, the microvasculatures derived from the isolated microvessels is adaptive, capable of acquiring an organotypic phenotype in the presence of tissue-specific parenchyma and stromal cells [24]. When implanted, microvessels rapidly inosculate with host vasculature to perfuse the implanted region [18, 19, 25, 26]. Recently, we have shown that stromal cells are important in guiding neovessels across tissue boundaries such as that present between a graft and the implant tissue [11]. Given these dynamics and vascularization capabilities, we hypothesized that isolated microvessel fragments would prove effective at vascularizing organoids.

To do this, we developed a simple protocol for co-seeding microvessels with mesenchymal stem cells (MSCs) in a self-assembled organoid format. MSCs are advantageous because they can be easily harvested and are conducive to creating patient-specific tissues and disease models. They can be differentiated into a variety of tissue types, including adipose, bone, smooth muscle, and cartilage [27–29]. MSCs are also highly pro-angiogenic [30], and others have shown that MSC organoids alone can increase tissue vascularization *in vivo* [31]. To demonstrate the versatility of our vascularization system and show its effectiveness in other tissues, we then incorporated microvessels into adipose-like organoids. Adipose plays a key role in several metabolic diseases, including diabetes and obesity [32, 33]. Better understanding the complex changes in function and signaling that occur in diseased states may accelerate development and testing of new treatment and therapies. Others have been developing adipose spheroids for this purpose, but, as discussed above, none have achieved the vascular complexity found *in vivo* [34–37]. As the vasculature plays such an essential role in most metabolic diseases [38], this component should not be ignored. Here, we demonstrated that microvessels can be used to fabricate functional, vascularized, adipose-like organoids.

2. Methods

2.1. Microvessel isolation

Microvessels were isolated from discarded human lipoaspirates, similarly to previously reported protocols [19, 20]. Briefly, adipose tissue is subjected to a limited collagenase digestion, followed by selective screening to remove remaining pieces of tissue and single cells. Each isolation of microvessels is subject to quality control testing, where angiogenic potential is assessed based on neovessel growth in a given amount of time. To reduce the effects of donor-to-donor variation, only lots with similar angiogenic potentials are used.

2.2. Cell culture

Bone marrow-derived human MSCs were purchased from Rooster Bio. Cells were expanded in DMEM/F12 (Gibco) with 10% fetal bovine serum (FBS; Gibco) in T75 flasks coated with 0.1% gelatin. After two passages, cells are used for MSC organoid formation, or differentiated into pre-adipocytes following previously described protocols, with slight modifications [39, 40]. Adipocyte differentiation medium (ADM) contained DMEM supplemented with 100 μM dexamethasone (Sigma), 0.5 mM (IBMX; Sigma), 100 μM indomethacin (Sigma), 5 μg ml^{-1} insulin (Sigma), and 0.5% FBS. Cells were cultured for 17 d, with medium changed every 2–3 d. On day 17, cells were either used for adipose-like organoid formation or continued in 2D culture. At this point, organoids or cells were switched to adipocyte maintenance medium (AMM). AMM contained 50:50 RPMI:DMEM supplemented with B27, 5 μg ml^{-1} insulin, 100 μM indomethacin, and 0.5% FBS. After 7 d of AMM, cultures were either fixed, flash frozen, or used for functional assays.

2.3. Transwell assay

Microvessels were plated in wells of a 24 well plate at a density of 100k ml^{-1} in 3 mg ml^{-1} collagen (Corning). MSCs were then trypsinized and resuspended in 3 mg ml^{-1} collagen at 900k cells ml^{-1} and pipetted into transwell inserts (270k cells well^{-1}). After the collagen gelled, transwell inserts with MSCs were moved into half of the microvessel containing wells of the 24 well plate, so microvessel growth with and without MSCs could be compared. Groups were tested in serum free microvessel medium containing DMEM/F12, 10 μg ml^{-1} insulin (Sigma), 100 μg ml^{-1} transferrin (Sigma), 30 nM sodium selenite (Sigma), 100 μM putrescine (Sigma), 20 nM progesterone (Sigma), and with or without the addition of 50 ng ml^{-1} vascular endothelial growth factor

(VEGF; Peprotech). Microvessels were cultured for 6 d prior to fixing overnight in 10% neutral buffered formalin (NBF; Fisher Scientific), with a medium change on day 4.

2.4. Organoid formation

MSCs or pre-adipocytes were trypsinized and resuspended at 2 million cells ml^{-1} (50k cells/organoid in all cases). In experiments containing microvessels, microvessels were mixed with the cell suspension prior to seeding. Then 25 μl of the combined suspension was seeded per organoid in a non-adherent V-bottom 96 well plate. In experiments evaluating the inclusion of collagen, a 3 mg ml^{-1} solution of collagen was prepared, and a volume was added to the cell suspension such that 30% of the total cell suspension volume was collagen. Microvessel incorporation was evaluated at microvessel:MSC ratios of 1:100, 1:50, 1:25, or 1:12.5. Subsequent experiments were all seeded using the 1:50 ratio (1k microvessels and 50k cells per organoid). All undifferentiated MSC organoids were cultured in our standard microvessel angiogenic medium, which contains RPMI supplemented with B27, 0.5% FBS, and 50 ng ml^{-1} VEGF. Adipose-like organoids were instead cultured in AMM. Culture medium was changed every 2 d.

2.5. Measuring angiogenic potential

Organoids were embedded in 3 mg ml^{-1} collagen after 2 or 5 d of culture. During embedded culture, angiogenic microvessels invade the collagen surrounding the organoid. After 2 d, the embedded organoids were fixed overnight in 10% NBF. After embedded organoids are cultured and fixed, they are stained with lectin as described below. The number of microvessels growing out of each organoid was counted and normalized to organoid circumference, measured in ImageJ. Organoid diameter was calculated from circumference.

2.6. Lipolysis assay

A lipolysis assay was performed on 2D (after 24 d of 2D culture) and 3D cultures (after 17 d of 2D and 7 d of 3D culture), using a commercially available kit (Sigma). Samples were treated with 1 μM isoproterenol for 4 h. For 2D cultures, supernatants were then mixed with the reaction solution and incubated according to manufacturer's instructions. For 3D cultures, organoids were homogenized in the supernatant after isoproterenol incubation using a plastic pestle, to release glycerol trapped inside the organoid. The homogenized sample was briefly centrifuged, and supernatants were used for the remainder of the manufacturer's protocol. Samples were read at 570 nm using a plate reader (BioTek Instruments). For 2D cultures, samples cultured in FBS were used as control samples that will not undergo lipolysis. For 3D samples, negative controls were not treated with isoproterenol.

2.7. Tumor necrosis factor alpha (TNF-α) challenge

Adipose organoids were seeded and cultured as described above. After 7 d of culture, medium was changed from AMM to AMM supplemented with or without 50 ng ml^{-1} TNF-α (Peprotech). The following day, organoids were either flash frozen for polymerase chain reaction (PCR) analysis, fixed for histology, or used for an interleukin-6 (IL-6) enzyme-linked immunosorbent assay (ELISA).

2.8. IL-6 ELISA

Organoids with and without microvessels and with or without TNF-α treatment were transferred with their supernatants to micro-centrifuge tubes and briefly homogenized with a plastic pestle. Samples were diluted and centrifuged for 2 min at 12 000 rcf to pellet remaining matrix and cell debris. An ELISA was performed with the supernatant following manufacturer instructions (R&D systems) to measure secreted IL-6 as a marker of adipocyte inflammation and dysfunction.

2.9. Histology and staining

Three-dimensional constructs were fixed overnight in 10% NBF at 4 °C, then permeabilized for 30 min with 0.25% Triton X-100, blocked overnight at 4 °C in 5% bovine serum albumin (BSA; Fisher Scientific), and stained overnight at 4 °C in a 1:50 dilution of rhodamine labelled UEA lectin (Vector Laboratories) in 5% BSA. After 30 min in Hoechst dye (1:3000 in DI water) at RT, constructs were washed a minimum of four times, with at least one overnight wash. Imaging was performed using a confocal Olympus FV3000 (organoid experiments) or an IN Cell 6500 high content analysis scanner (Cytiva; transwell experiment). Additional phase contrast images were taken of transwell constructs with an Olympus CKX53 inverted microscope.

Additional fixed organoids were stained with a BODIPY™ 493/503 (4,4-Difluoro-1,3,5,7,8-Pentamethyl-4-Bora-3a,4a-Diaza-s-Indacene) dye (Invitrogen). After permeabilization and blocking as described above, dye was added to organoids at a 1:100 dilution in 5% BSA. After 30 min, organoids were rinsed multiple times with PBS and imaged on an IN Cell analyzer 6500 HS (Cytiva).

Fixed, non-collagen embedded organoids were sent out for processing, paraffin embedding, and sectioning (Saffron Scientific). Slides were deparaffinized and rehydrated to water prior to staining with Harris Hematoxylin (Sigma) and Eosin (Sigma) to visualize morphology or picrosirius red (Sigma) to visualize collagen with fast-green counterstain (Sigma).

Two-dimensional cell cultures were fixed for 30 min at RT in 10% NFB, incubated with 60% isopropyl alcohol for 5 min, and then Oil Red O (Sigma) for 15 min. Samples were rinsed thoroughly in 60% isopropyl alcohol and then water. A Meyer's

Table 1. Primer sets used for PCR.

Gene	Primer sequence
Adiponectin forward	5′-AAGGAGATCCAGGTC TTATTGG-3′ [41]
Adiponectin reverse	5′-ACCTTCAGCCCCGGGTAC-3′ [41]
PPAR-γ forward	5′-CATAAAGTCCTTCCCGCTGA-3′ [37]
PPAR-γ reverse	5′-GGGGGTGATGTGTTTGAACT-3′ [37]
IL-6 forward	5′-GGTACATCCTCGACGGCATCT-3′ [42]
IL-6 reverse	5′-GTGCCTCTTTGCTGCTTTCAC-3′ [42]
Insulin receptor forward	5’-TGCAAACCCAAGAACGTCAG-3’
Insulin receptor reverse	5’-AGCTTCCGGGAGTTCAGTAC-3’

Hematoxylin stain (Sigma) was used for 15 min followed by additional PBS washes and imaging on an Olympus CKX53 microscope.

2.10. Image analysis

Phase contrast images of microvessels used for the transwell assay were analyzed using the BioSegment™ Software Application (Advanced Solutions). The software uses machine learning to identify and quantify microvessel length in an image. Briefly, a fraction of images was annotated ‘by hand’, where the user identified and marked individual vessels. From this information, the program ‘learned’ the identifying features of a microvessel and accurately identified vessels from the remainder of the images and provided microvessel length for each image. Lengths calculated from each image (minimum of six per well) within a single well were added together, to yield a length value for each well. Three wells were averaged for each group, to provide average microvessel length under each treatment condition.

2.11. Polymerase chain reaction (PCR)

Ribonucleic acid (RNA) was extracted from either 2D cultures or 3D organoids using a Qiagen RNeasy Plus Micro kit following manufacturer’s protocols. RNA was converted to complimentary deoxyribonucleic acid (cDNA) with SuperScript™ IV VILO™ Master Mix (Fisher Scientific). cDNA was amplified with human primers (IDT Technologies) listed in table 1. Primers for insulin receptor were designed using Primer3 software (NIH) and verified using BLAST database (NIH), with gene coding obtained from GenBank (NIH).

Real-time PCR (RT-PCR) was performed using a SYBER master mix (Fisher Scientific) and CFX96 Real Time System (Bio Rad). Adiponectin and peroxisome proliferator-activated receptor gamma (PPARγ) expression were normalized to Glyceraldehyde 3-phosphate dehydrogenase (GAPDH) (IDT Technologies) and compared to either FBS treated controls (2D) or organoids without microvessels (3D). After RT-PCR, amplified cDNA was loaded into a 2% agarose gel and run at 90 V. Gels were imaged for SYBER green on a gel scanner (Azure Biosystems).

2.12. Statistical analysis

Statistics were performed using SigmaPlot 11.0 (Systat). Where applicable, one-way ANOVA tests were performed with a Newman–Keuls post hoc analysis, or a student’s t test. For all comparisons, the significance level $\alpha = 0.05$.

3. Results

3.1. MSCs promote angiogenesis

To evaluate the effect of MSCs on angiogenesis from the isolated microvessels, MSCs were embedded in collagen and placed on top of a transwell insert, while microvessels were cultured in collagen on the well plate surface, below the insert. Groups were tested in a standard serum-free medium used by our lab to culture human microvessels, both with and without exogenous VEGF. Microvessels cultured with either MSCs or VEGF had significantly increased vascular growth (figures 1(A)–(D)). The inclusion of MSCs increased vessel density comparably to exogenous VEGF alone (figure 1(E)). Additional lots of MSCs from different donors subjectively yielded similar increases in microvessel growth when compared to controls without MSCs (supplementary figure 1 (available online at stacks.iop.org/BF/13/035022/mmedia)).

3.2. Microvessels form vascular networks within MSC organoids

Microvessels were mixed with MSCs to create organoids at ratios of either 1:100, 1:50, 1:25, or 1:12.5 microvessels:MSCs. Organoids embedded in collagen at day 5 and fixed on day 7 showed robust angiogenic outgrowth and network formation (figures 2(A)–(D)). The number of neovessel sprouts growing out of each organoid into the surrounding matrix was quantified and normalized to organoid circumference (figures 2(E) and (F)). Organoids with the highest concentration of microvessels (1:12.5) were challenging to image, as most of the organoid appeared to consist of lectin positive cells, making it impossible to distinguish vessels within the organoid. Outgrowths in the 1:12.5 group were subjectively shorter than those in the other groups, and these organoids had the largest diameter (figure 2(F)). Both the 1:100 and 1:12.5 had significantly lower numbers of angiogenic outgrowths than 1:50 or 1:25. Between the 1:50 and 1:25 groups, the vascular network in the 1:50 ratio appeared more distinct throughout, with longer outgrowths. Organoids embedded at an

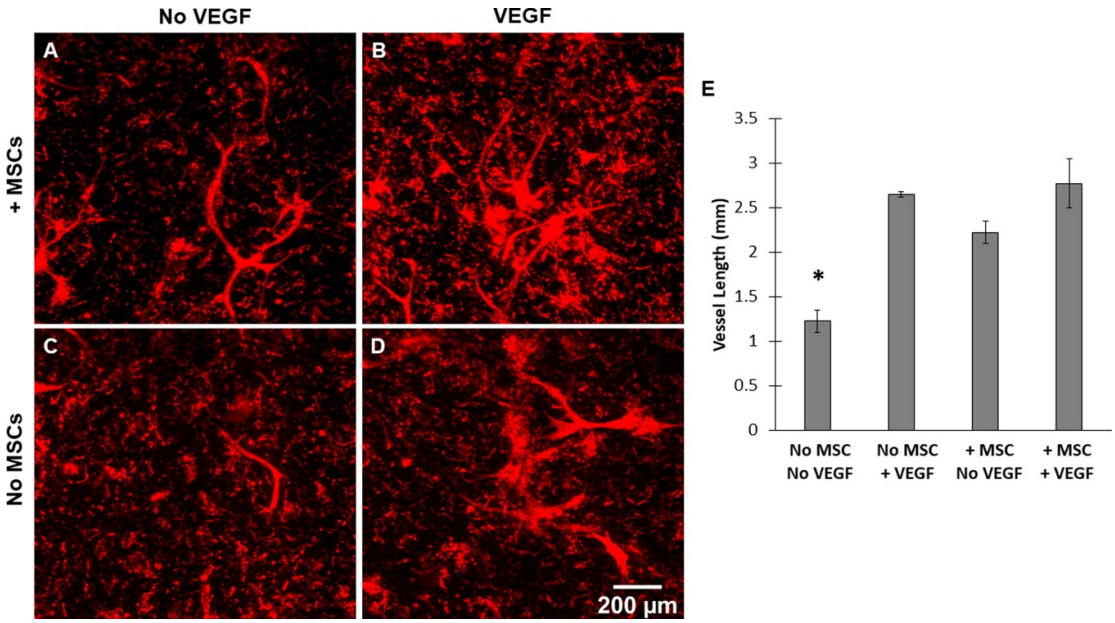

Figure 1. MSCs stimulate angiogenesis. Microvessels were either co-cultured with MSCs in transwell inserts (A) and (B), or without MSCs (C) and (D). Culture mediums either contained no VEGF (A) and (C), or 50 ng ml^{-1} VEGF. Wells with lectin stained microvessels (red = endothelial cells) were scanned with a confocal microscope and processed with the BioSegment software package to quantify microvessel length density in each well. Average vessel densities for each group are shown in (E) after 6 d of culture. $N = 3$, bars are mean ± SD. $^{*}P < 0.05$ compared to all other groups, one-way ANOVA with Newman–Keuls post hoc test.

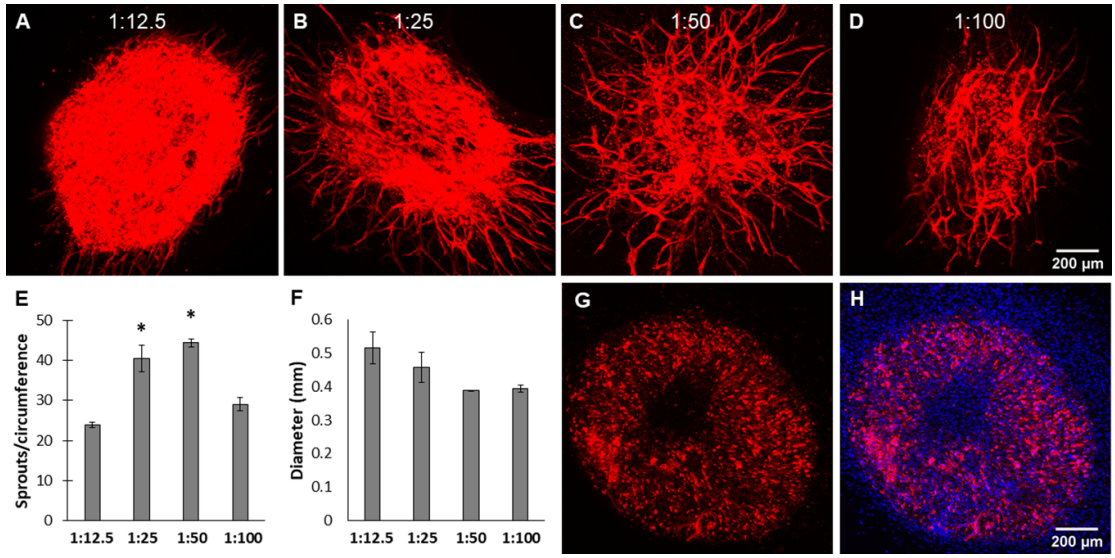

Figure 2. Vascularized MSC organoids. MSCs and microvessels were mixed and seeded at microvessel:MSC ratios of 1:12.5 (A), 1:25 (B), 1:50 (C), or 1:100 (D). The number of sprouts growing out of each organoid into the surrounding collagen matrix was counted and normalized to the circumference of the organoid (E) and (F). (A)–(D) were taken after a total of 7 d of culture (5 d as organoids alone, 2 d as organoids embedded in collagen). An earlier timepoint is shown in (G) and (H), where organoids are embedded at day 2 and fixed and stained at day 4 (1:50 group shown). Red = lectin (endothelial cells), blue = Hoechst (nuclei), scale = 200 μm. One way ANOVA with Newman–Keuls post hoc test. $^{*}P < 0.05$ compared to both 1:12.5 and 1:100, $N = 3$, bars are mean ± SD.

earlier time point, day 2, showed limited angiogenic growth when analyzed at day 4, although incorporated fragments are still visible (figures 2(G) and (H); 1:50 group shown). This was not surprising, as microvessels embedded in collagen typically do not show robust growth until around days 5–7. Interestingly, we observed some correlation between organoid size and vascular potential, suggesting that the lower angiogenic potential in organoids with more microvessels may be due, in part, to their larger size (squared correlation coefficient = 0.597, supplementary figure 2). A cross section of the organoid is shown in supplementary figure 3, where vessel lumens can be seen throughout the construct.

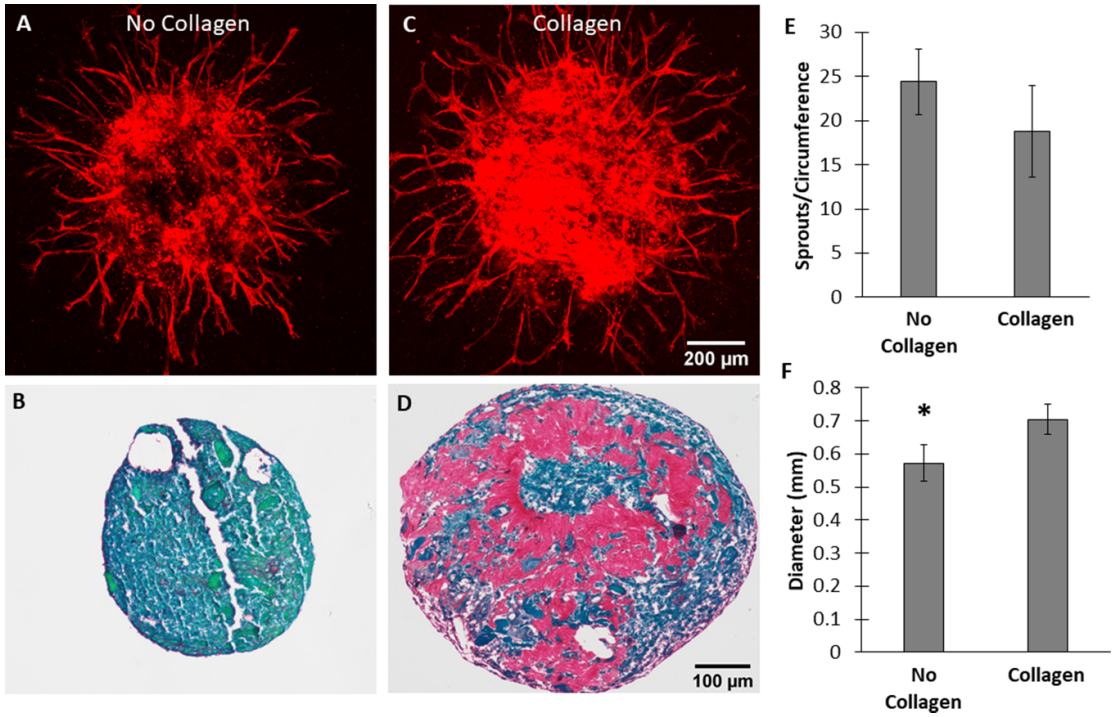

Figure 3. The effects of collagen incorporation on organoid vascularization. Organoids were seeded without collagen (A) and (B), or with collagen (C) and (D), in the seeded cell suspension. Vascularization can be clearly seen in confocal images of embedded organoids ((A) and (C) lectin stain, red = endothelial cells). A picrosirius red/fast green stain shows collagen remaining in MSC organoids after 7 d of culture ((B) and (D) red = collagen, green = counterstain). The number of angiogenic sprouts growing out the organoids were not significantly different between the two groups (E), although organoids with collagen maintained a larger diameter (F). Student's t-test, $^{*}P < 0.05$, bars are mean ± SD, $N = 6$–7.

3.3. Collagen is not necessary for vascular network formation in organoids

Initially, collagen was included in organoid fabrication protocols, as we have previously observed that microvessels need a fibrillar matrix to grow and survive. However, we also explored organoid fabrication without collagen in efforts to increase cell densities. Compared to organoids made without collagen (figures 3(A) and (B)), the presence of collagen (figures 3(C) and (D)) did not have a significant effect on angiogenic growth (figure 3(E)). Picrosirius red/fast green staining of organoid sections showed that collagen remained in collagen-formed organoids after 7 d of culture, although its distribution was uneven throughout the organoid (figure 3(D)). This likely contributed to overall larger diameters observed in organoids with collagen (figure 3(F)). In this group, there is a small amount of collagen around the organoid edges that is much less dense and likely secreted by cells. Interestingly, however, less of this cell-secreted collagen was visible in organoids where collagen was not included in initial fabrication (figure 3(B)).

3.4. MSC derived pre-adipocytes can be maintained in angiogenic medium

Towards fabricating adipocyte-organoids, we developed a protocol using staged culture media to support differentiation of MSCs into pre-adipocytes while promoting microvessel growth. This protocol, and development of AMM, was necessary, as standard ADM did not support microvessel growth (supplementary figure 4). In this protocol, MSCs are cultured in 2D with ADM to induce differentiation towards adipocytes. Then, these committed MSCs are combined with isolated microvessels to form the organoid. Organoids are then cultured in AMM, which supported both MSC differentiation and microvessel angiogenesis. To verify that AMM maintains an adipogenic phenotype, some wells after 17 d were switched to AMM for an additional 7 d, while others were maintained in ADM. Subjectively, more lipid droplets were visible after culture in AMM, compared to 24 d in ADM (figures 4(A) and (B)). Control MSCs cultured in FBS expansion medium had no lipid droplets visible (figure 4(C)). A lipolysis assay was performed at day 24 as a measure of adipocyte function. Cells cultured in AMM after ADM commitment had a significantly higher glycerol release than cultures continued on ADM or on FBS-containing medium (figure 4(D)). RT-PCR was performed to measure relative expression of adiponectin and PPARγ, markers typically associated with mature, functional adipocytes. Adiponectin was expressed in cells cultured in ADM and AMM, but not FBS (figure 4(E)). RT-PCR yielded nearly identical delta delta Cq values for ADM and AMM, suggesting comparable upregulation in both

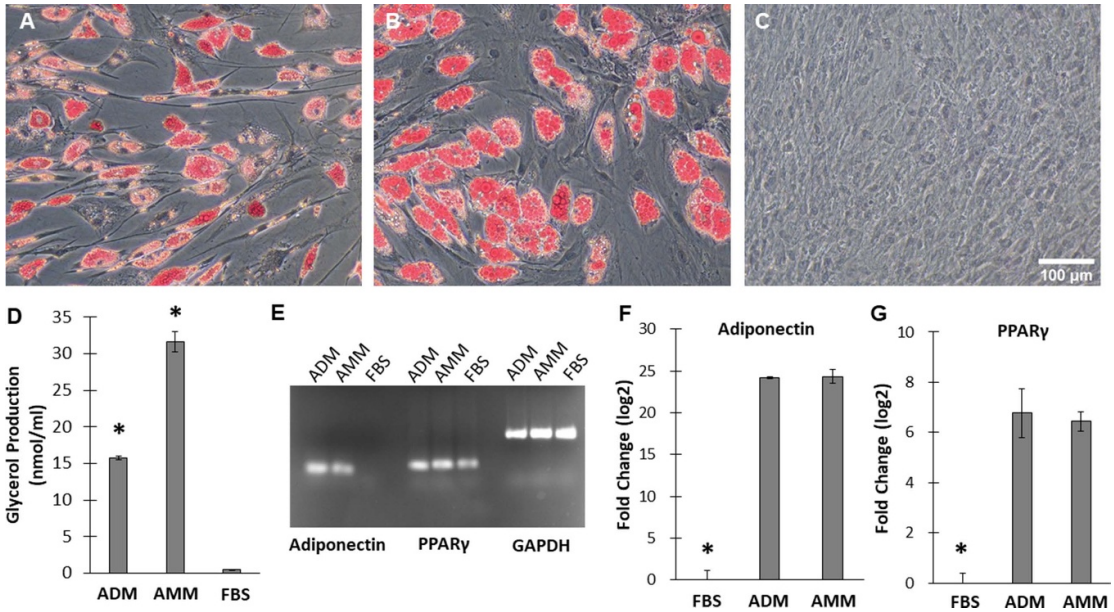

Figure 4. 2D cell cultures after differentiation. Oil Red O staining with a hematoxylin counterstain shows lipid droplets (lipids = red, nuclei = purple) in cells treated with ADM for 24 d (ADM; (A)), treated with ADM for 17 d, then AMM for 7 d (AMM; (B)), or were cultured in 10% FBS (FBS; (C)). A lipolysis assay shows glycerol production in response to isoproterenol in each of the three treatments (D). PCR gel shows expression of adiponectin, PPARγ, and GAPDH (E). RT-PCR shows comparable expression of both adiponectin (F) and PPARγ (G) in both ADM and AMM groups, which are compared to FBS. $^{*}P < 0.05$ compared to all other groups, one-way ANOVA with Newman–Keuls post-hoc analysis. $N = 3$. Bars are mean ± SD.

groups compared to FBS (figure 4(F)). PPARγ was expressed in all three groups (figure 4(E)), although PPARγ expression was substantially upregulated in both ADM and AMM when compared to FBS controls (figure 4(G)).

3.5. Vascularized adipose-like organoids can be formed from MSC derived pre-adipocytes

Adipose-like organoids were formed with MSCs that had differentiated for 17 d in ADM with or without the inclusion of microvessels at the time of organoid formation. In initial experiments, collagen was included in organoid fabrication. Organoids were then cultured for 7 d in AMM (with some embedded in collagen on day 5). Paraffin sections stained for hematoxylin and eosin suggested that cells had differentiated into mature adipocytes due to the many voids in the tissue where lipid droplets were extracted during processing (figures 5(A) and (B)). Mature adipocytes were also visible in images of whole organoids stained with BODIPY dye (figure 5(C)). Cells in organoids without microvessels did not remodel the collagen, but instead separated from the collagen into cell-dense regions, leading to larger organoids (figure 5(A)). Interestingly, in organoids with microvessels, the collagen was remodeled, resulting in a compact, cell dense organoid (figure 5(B)). Still, voids from large lipid droplets are visible, primarily in the organoid center but also spread throughout the collagen. Lectin staining of embedded, whole adipocyte organoids showed highly branched vascular networks growing throughout organoids with incorporated microvessels. When the organoids were placed in a collagen bed, vessel growth was largely contained within the adipocyte organoids, with fewer numbers of angiogenic sprouts invading the surrounding collagen matrix than in MSC experiments (figures 5(D) and (E)).

The experiment was repeated without the inclusion of collagen in organoid fabrication, as we had concerns that the large diameter of organoids with collagen and no microvessels would adversely affect adipocyte function, due to diffusion limitations, independently of microvessel inclusion. Morphologically organoids without collagen without and with microvessels looked similar (figures 6(A) and (B)). Microvessels can be seen growing out of embedded organoids (figures 6(D) and (E)), although they are fewer in number and have a thinner neovessel morphology than with collagen inclusion. Organoids without collagen were used in subsequent PCR and functional tests.

Organoids with and without microvessels produced glycerol in response to isoproterenol, a measure of lipolysis. Those with microvessels produced slightly more glycerol, although this difference was not significant (figure 7(A)). Both groups of organoids expressed the adipocyte markers adiponectin and PPARγ (figure 7(B)). RT-PCR showed no meaningful difference in expression of these markers in organoids with microvessels when compared to organoids without microvessels (figures 7(C) and (D)).

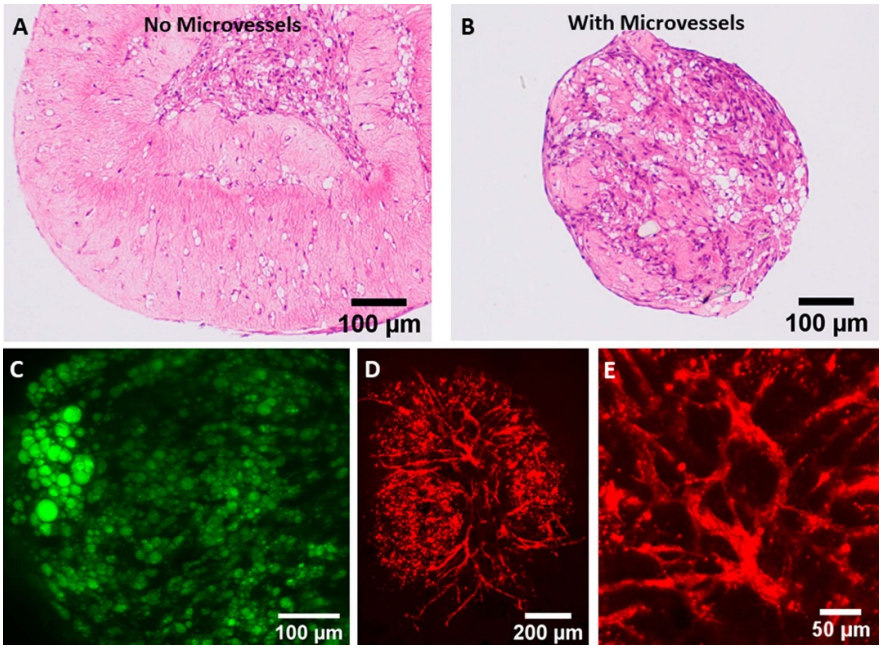

Figure 5. Vascularized adipose-like organoids with collagen inclusion. H&E stain of organoids seeded with collagen and pre-adipocytes, without microvessels (A), or with microvessels (B), after 7 d of culture in AMM. Fluorescent BODIPY stained image shows apparently mature adipocytes within MV containing organoid, characterized by large round lipid droplets (C). After 2 d of embedded culture (7 d total organoid culture), microvessels can be seen growing throughout the organoid ((D) (E); lectin stain, red = endothelial cells). (E) is a high magnification inset of (D).

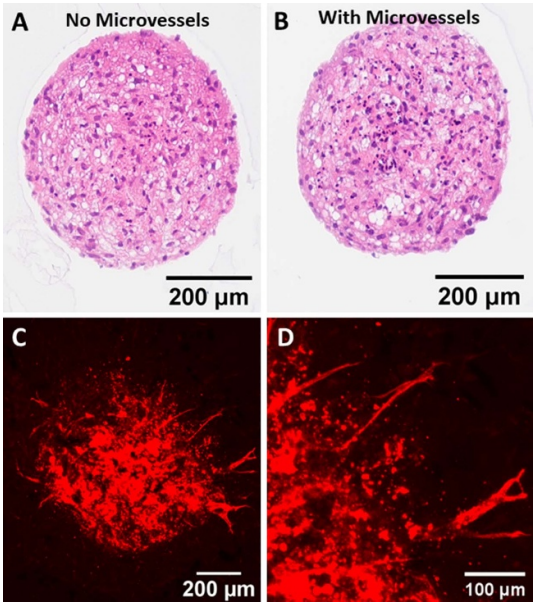

Figure 6. Vascularized adipose-like organoids without collagen inclusion. H&E stain of organoids seeded with pre-adipocytes but no included collagen, either without microvessels (A), or with microvessels (B), after 7 d of culture in AMM. After 2 d of embedded culture (7 d total organoid culture), some neovessel sprouts can be seen growing out of the organoid into the surrounding matrix ((C) and (D); lectin stain, red = ECs). (D) is high magnification inset of (C).

3.6. Adipocytes upregulate insulin receptors in the presence of microvessels

Insulin exerts important functional control of adipocytes, signaling via the insulin receptor [43]. To further evaluate the effect of microvessels on adipocyte function, we performed PCR to examine insulin receptor expression. Organoids with microvessels had a three-fold (log2) increase in insulin receptor expression compared to organoids without microvessels (figure 8(A)). Insulin receptor expression occurred primarily on the surface of adipocytes throughout the construct, with the included microvessels showing relatively low insulin receptor expression (figure 8(B)).

3.7. Microvessels modulate adipose-like organoid secretion of IL-6 in response to TNF-α

Adipose inflammation, often modeled with exposure to TNF-α, is a hallmark feature of adipose dysfunction [44]. To explore this, adipose-like organoids with and without microvessels were treated with TNF-α for approximately 24 h followed by measurement of IL-6, an inflammatory cytokine known to increase in response to TNF-α treatment in adipocytes [45]. Without TNF-α, IL-6 was almost nonexistent in samples without microvessels but was present at low levels in organoids with microvessels. Organoids treated with TNF-α had dramatically increased IL-6 secretion, although less was secreted by organoids with microvessels than those without (figure 9(A)). Interestingly, IL-6 expression in both TNF-α treated groups was comparable, suggesting the microvessels caused a difference in IL-6 secretion (figure 9(B)).

In contrast, PPARγ expression was not affected by the presence of microvessels when microvessels were present in response to TNF-α (figure 9(C)).

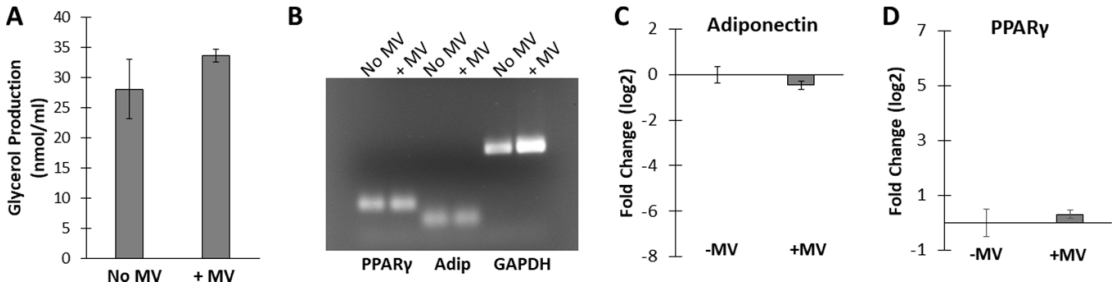

Figure 7. Adipose organoid function. Lipolysis assay showing glycerol production in organoids in response to isoproterenol treatment (A). PCR shows expression of PPARγ, adiponectin, and GAPDH in both groups (B). RT-PCR shows relative expression of adiponectin (B) and PPARγ (C) in organoids with microvessels compared to organoids with no microvessels. $P > 0.05$, student's t-test.

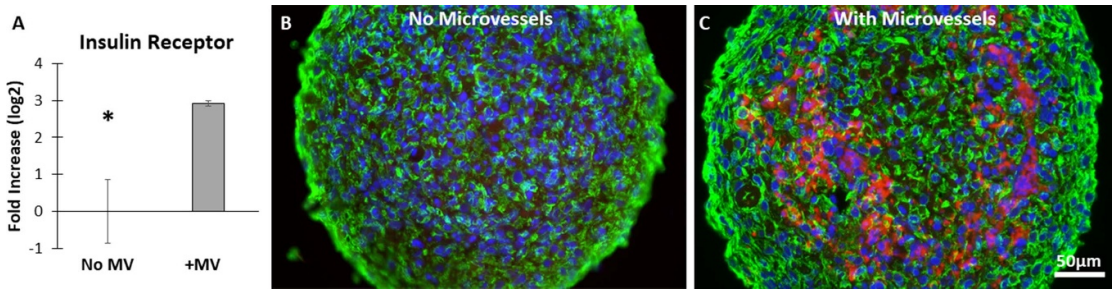

Figure 8. Microvessel effect on insulin receptor expression. RT-PCR indicated microvessels (MV) increase insulin receptor expression compared to organoids without microvessels (A). IHC shows receptor expression in organoids without (B) and with (C) microvessels. Green = insulin receptor, red = endothelial cells (lectin), blue = nuclei (Hoechst); scale = 50 μm. $^*P < 0.05$, student's t test.

Adiponectin expression changed minimally in groups with no microvessels in response to TNF-α and with microvessels and no TNF-α. A small but distinct downregulation was visible in organoids with microvessels following TNF-α treatment (figure 9(D)).

4. Discussion

Here, we developed human, vascularized, adipose-like organoids for use in adipose tissue modeling. Our strategy entailed using isolated human microvessels, which are intact pieces of microvessels comprised of a spectrum of cell types, as the source of vascular elements to better reconstitute the adipose tissue environment. Furthermore, we explored the inclusion of type I stromal collagen in fabricating the organoids as a provisional stromal matrix to support tissue formation and maturation. Our results indicate that including microvessels in adipose-like organoids can be beneficial towards recapitulating native adipose tissue *in vitro*, regardless of collagen inclusion. With collagen, a robust neovascular network capable of further angiogenesis outside of the organoid was formed along with mature adipocytes. This approach would be ideal for constructs intended for implantation or therapeutic use, as this neovascular network will likely rapidly inosculate with the host vasculature to provide perfusion. For *in vitro* screening, vascularized organoids fabricated without collagen were smaller and more consistent. While less capable of outward angiogenesis into a surrounding matrix, the microvessels in organoids without collagen led to a more dynamic adipose-like tissue environment, particularly related to adipose inflammation and insulin signaling.

The integration of the microvessels with the adipocyte precursors required the development of a staged approach to simultaneously facilitate adipocyte differentiation and angiogenesis. This need arose from early observations that the media commonly used to differentiate stem cells into adipocytes inhibits angiogenesis. Combining ECs alone with pre-adipocytes can enhance adipocyte differentiation [46] or cause adipocyte de-differentiation [47, 48], likely reflecting differences in derivation protocols. Indeed, Lai *et al* observed that the pre-adipocyte:HUVEC ratio played a large role in pre-adipocyte function, with lower concentrations of HUVECs causing a larger increase in triglyceride content per adipocyte [46]. Thus, our findings indicate that our organoid fabrication protocol, with or without microvessels, consistently produces differentiated adipocytes while enabling the addition of other elements such as stromal matrix, depending on the application. Furthermore, this strategy accommodates the use of primary cell sources, MSCs and human microvessels, to potentially capture more accurate biology and even

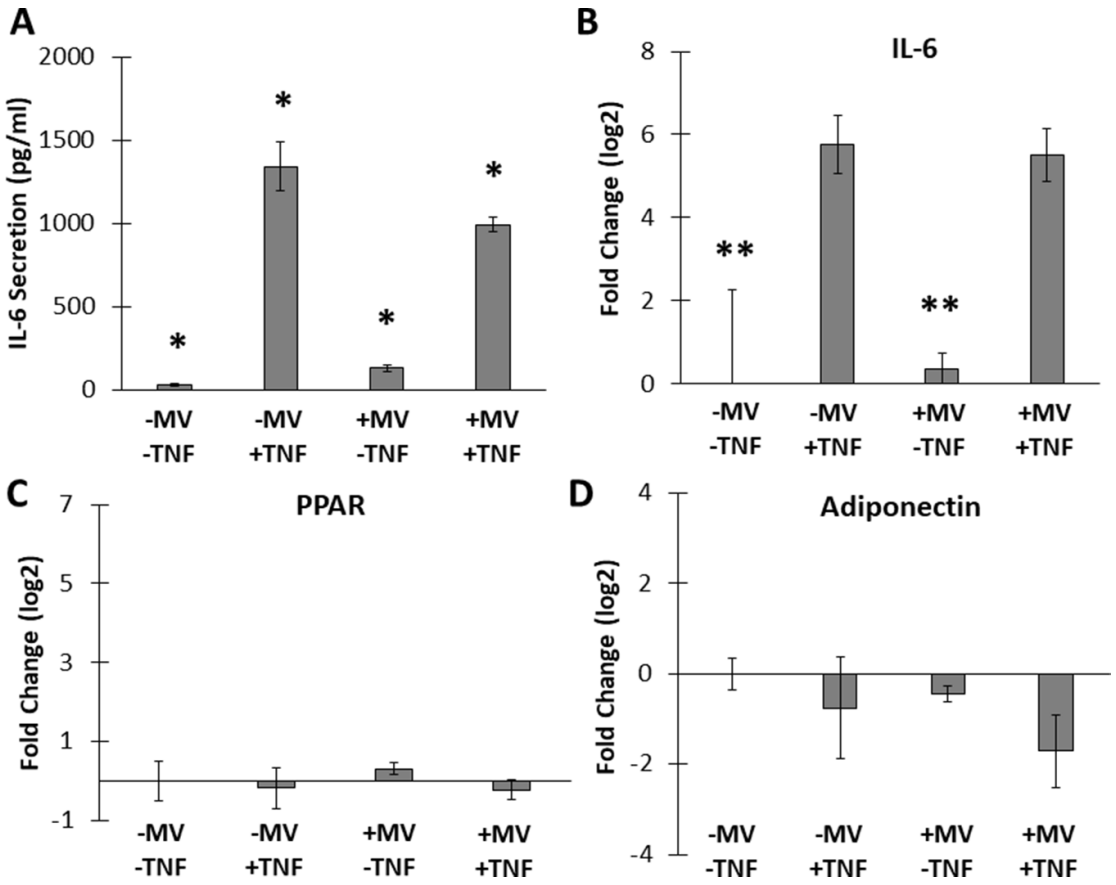

Figure 9. TNF-α challenge. Organoids with and without microvessels were treated with or without TNF-α for 24 h. An ELISA was used to measure secretion of the inflammatory cytokine IL-6 (A). PCR shows the effect of TNF-α on IL-6 gene expression (B) and the adipocyte markers adiponectin and PPARγ (C) and (D). $^{*}P < 0.05$ compared to all other groups. $^{**}P < 0.05$ compared to groups with TNF-α treatment. One-way ANOVA on ranks with Newman–Keuls post hoc analysis (A), or one-way ANOVA with Newman–Keuls post hoc analysis (B)–(D).

enable personalized medicine-related uses. To mitigate the complications due to biological heterogeneity intrinsic to donor populations, we developed tests for the MSCs and microvessels enabling us to qualify donor lots by desired functional outcomes. For the MSCs, we tested their ability to enhance angiogenesis, and microvessels we tested angiogenic potential. Thus, we used only MSC and microvessel donor lots with comparable functional outcomes throughout the project. Of course, despite the challenges of donor variation, depending on the application, this heterogeneity can be leveraged to pursue new insights into the variations of adipose biology in the healthy and diseased populations.

In developing the fabrication methods, we first examined the effects of MSC co-culture on microvessel growth. Isolated microvessels and MSCs were cultured in the same well using a transwell insert, which physically separates the MSCs and microvessels, but allows molecule exchange between the respective media compartments. MSCs secrete a host of angiogenic growth factors, including VEGF, fibroblast growth factor (FGF), insulin-like growth factor (IGF), hepatocyte growth factor (HGF), and many others [49]. Therefore, it was not surprising that groups with MSCs produced a higher vessel density than groups without MSCs. This effect was comparable to exogenous high concentrations of VEGF (50 ng ml^{-1}), which is typically used to stimulate angiogenesis (figure 1). This lot of MSCs produced 467 pg 10^5 cells d^{-1} of VEGF (as determined by the manufacturer). Meaning that after 4 d of culture, assuming a 24 h MSC doubling time, 3.72 ng of VEGF is produced in 1.8 ml of medium, which is substantially less than in groups treated with exogenous VEGF. This indicates that the combination of multiple growth factors, albeit in smaller concentrations, released into the medium by the MSCs is more effective than high doses of VEGF alone. This may have larger implications for development of future microvessel-containing tissues, as many tissue systems may not respond well to high doses of growth factors. For example, VEGF is inhibitory of adipocyte differentiation [50]. If MSCs can be added to a tissue construct and produce comparable or improved angiogenesis over VEGF, it widens the number of potential applications for the microvessel vascularization system.

Visualizing angiogenesis within the organoids was challenging due to difficulties in distinguishing

neovessels within the organoid. Thus, we developed a functional assay to assess angiogenic potential of the microvessels, as an indicator of microvessel presence and function, within the organoids. To do this, we embedded the organoids in a collagen matrix and quantified angiogenic sprouts growing out of the organoids into the matrix. We previously used a similar method to model vascularization across tissue interfaces [11], as have others to assess angiogenic potential of EC co-culture organoids [51, 52]. Within 48 h we observed rapid vessel outgrowth from the vessels into the surrounding collagen (figure 2). In addition to demonstrating functional integrity of the neovasculatures in the organoids, the robust outgrowth of neovessels into the surrounding matrix suggests that, if implanted, these organoids will rapidly inosculate with the surrounding host circulation.

Interestingly, angiogenic growth depended on the ratio of microvessels:MSCs within the organoid. When microvessels were seeded at higher numbers, fewer angiogenic sprouts were observed crossing into the collagen matrix (figure 2). It is possible that having too many vessels inhibited neovessel growth and/or promoted microvessel disassembly into single cells. Additionally, differences in mixed cell densities may alter cell competition dynamics, as is often described in tumor-modeling and stem-cell organoids [53], leading to instability of the microvessels. Alternatively, the larger size of the organoids in this group may be affecting vascularization dynamics. Comparing organoid vascularity and diameter suggests an optimal size threshold of 400 μm: increasingly larger organoids above this threshold limits vascularization while organoids below this threshold, regardless of size, supported vascularization. Bhang *et al* showed that organoids with diameters ranging from 200 to 400 μm produced more angiogenic growth factors than organoids of other sizes [31]. Perhaps a similar dynamic is occurring in the organoids in the present study.

It is likely that larger organoids experience necrosis due to limitations in oxygen and nutrient diffusion. Given that the average diameter of the 1:12.5 group was approximately 500 μm, some functionality may have been lost due to necrosis. The 1:50 and 1:100 groups were just under 400 μm, while 1:25 was just above this threshold. Both the 1:50 and 1:100 groups had comparable numbers of sprouts growing out the organoid, although 1:50 subjectively had a more robust vascular network throughout. The 1:100 had fewer sprouts, likely due to the overall lower number of microvessels. To further explore this, we plotted vascularity and diameter of organoids from all MSC experiments on a single graph (supplementary figure 2). There is a correlation, particularly above 500 μm, although an R^2 value of 0.597 suggests it is likely not the sole contributing factor.

In initial experiments, a small amount of collagen was included in organoid seeding. This is because we have previously observed that microvessels require a fibrillar 3D environment to maintain native microvessel structure and undergo angiogenesis. We hypothesized that this initial collagen incorporation would help maintain microvessels until MSCs secreted their own collagen and remodeled the organoid microenvironment. In all experiments, seeded cell/collagen suspensions rapidly contracted into a tight organoid within 24 h. However, the addition of collagen to an organoid may not be feasible in all cell systems, particularly with cells that do not rapidly remodel collagen. Thus, we decided to do a formal comparison of MSC organoids with and without collagen. Surprisingly, robust angiogenesis and neovascular network formation occurred whether collagen was included or not (figure 3). This indicates that other matrix components are providing enough structure to support microvessel growth. After 7 d of culture, collagen was still clearly visible in histological sections of the organoids, although it was largely in clumps that were unevenly distributed throughout the organoid. Thus, while some remodeling is evident, MSCs did not completely remodel the initially seeded collagen within the 7 d period. Almost no collagen was observed in organoids that did not contain collagen in the initial seeding suspension, suggesting that limited collagen is being produced by MSCs. Overall, this experiment showed that microvessels are capable of robust angiogenesis with or without collagen in organoids. Thus, whether to include collagen or not should be decided based on the application. Organoids that need to be handled early in culture may benefit from the added extracellular matrix, while those with cell types that require a higher cell density or smaller organoid size do not need it.

Next, we incorporated microvessels into adipose-like organoids. One of the challenges in creating a multi-cell type organoid is finding an appropriate culture medium to support the phenotype and function of all cellular components. In preliminary studies, we observed that IBMX, which is commonly used to induce pre-adipocyte differentiation, permanently impeded microvessel growth (supplementary figure 4). Thus, we developed a protocol with two different medium types that are used in stages. An induction medium (ADM) was used to stimulate MSC differentiation to pre-adipocytes and a maturation medium (AMM) was used to maintain and continue their differentiation while supporting microvessel growth. Qian *et al* also utilized a maintenance medium for pre-adipocytes, although this consisted only of DMEM and insulin, which is unlikely to support microvessel growth [40]. Here, we used both insulin and a standard B27 supplement in an RPMI:DMEM 50:50 mix. B27 and RPMI strongly support microvessel growth (supplementary figure 4), so we combined these supplements with DMEM and insulin, which support pre-adipocyte

differentiation. This new medium, AMM, resulted in microvessel growth comparable to our control serum free medium (supplementary figure 4). With the staged treatment protocol, cells had more, and larger lipid droplets visualized with Oil Red O staining than ADM treatment alone. Additionally, cells treated with AMM produced higher glycerol amounts when stimulated with isoproterenol (figure 4). These results suggest that our staged medium treatments differentiated cells further towards mature adipocytes than ADM alone.

Acosta *et al* also used a staged medium to derive adipocytes from whole rat microvessels [54]. Because isolated microvessels contain resident stem cells in the microvessel wall, adipocytes formed spontaneously from microvessels alone. Similarly to our findings, the authors found that the timing of angiogenic growth medium and ADM was critical, although in their study, differentiation medium reduced angiogenesis and growth medium reduced differentiation [54]. In our study, perhaps reflecting different media compositions, we did not see any decrease in pre-adipocyte differentiation with the pro-angiogenic AMM, although less neovascular network formation was visible compared to organoids fabricated from undifferentiated MSCs.

As with the MSC organoids, we initially included collagen in the fabrication of adipose-like organoids to facilitate microvessel growth and neovascular network formation. Interestingly, organoids with microvessels remodeled and compacted collagen, but organoids without microvessels did not. Instead, cells seemed to largely separate out from the collagen, giving the appearance that the collagen was encasing the organoid, with only a small number of cells throughout the collagen (figure 5). This resulted in extremely large organoid diameters (>800 μm), which may limit oxygen and nutrient diffusion to the center of the organoids and impair function. Because of this, the experiment was repeated without collagen, and these replicates were used for all functional testing and PCR. Interestingly, we observed that when collagen was included in adipose-like organoids, microvessels grew throughout the organoid and adopted a more mature morphology. This can be clearly seen in figure 5, where vessels are wider, contain more branch points, and are more interconnected than those seen in MSC organoids (figure 2). In separate experiments without collagen, there were a limited number of microvessels growing out of the organoid, and those present had a thin, sprout-like morphology that is much less mature (figure 6). These findings contrasted with our earlier experiments in the MSC organoids, where the presence of collagen did not affect microvessel outgrowth (figure 3). This difference may reflect the pro-angiogenic environment established by the MSCs versus a more stable environment established by more mature adipocytes. It should also be noted, that, while we have seen this reduced angiogenesis in adipose-like organoids without collagen in multiple experiments, microvessel donor-to-donor variation cannot be completely excluded as different microvessel lots were used in these experiments (despite microvessel qualification tests).

We hypothesized that the microvessels, which are comprised of multiple cells types, would influence the organoids towards a more native-like adipose tissue environment. While base-line adipocyte function (e.g. marker expression and lipolysis) in the organoids was not substantially affected by the presence of microvessels, indicators of adipose tissue dynamics were. Inclusion of microvessels significantly increased insulin receptor expression in adipocytes. Insulin signaling, via its receptor, is important in adipocyte energetics, causing adipocytes to take up glucose and free fatty acids while reducing lipolysis [43]. While beyond the scope of this study, it would be interesting to explore the dynamics between insulin signaling and inflammatory signals. Furthermore, the vascularized adipose organoids should be amenable to experiments addressing insulin resistance as the significant baseline presence of insulin receptors creates a more dynamic range in insulin responses.

The microvessels also modulated the complex dynamics of cytokines regulating adipose function. TNF-α plays a critical and complex role in adipose disease and dysfunction [55, 56]. Exposure to TNF-α induces adipocytes to secrete cytokines, such as IL-6, which, in turn, also regulate adipocyte biology [45]. As expected, we observed increased IL-6 secretion by organoids with and without microvessels when acutely challenged with TNF-α. However, less IL-6 protein was secreted by organoids fabricated with microvessels in response to TNF-α, despite relatively equal levels of IL-6 transcript, suggesting a more complex regulatory dynamic. Whether or not this reflects a less inflammatory condition is less clear. While IL-6 is best known for increasing inflammation, IL-6 can either increase or decrease adipose tissue inflammation, depending on the cell source [57]. If secreted by adipocytes, IL-6 increases inflammation. But if secreted by myeloid cells, it has the opposite effect, and was found to decrease inflammation and lessen glycemia and insulin resistance in mice [57]. Interestingly, organoids with microvessels expressed a higher baseline level of IL-6 than those without. IL-6 is produced by a variety of cell types in non-stimulated conditions [58], including those present in mature microvessels. Perhaps this baseline production of IL-6 and differences in IL-6 secretion in response to TNF-α is due to these other cells types introduced via the microvessels, including ECs and macrophages. Additionally, healthy adipocytes can secrete low levels of TNF-α during normal remodeling [59] and during lipolysis [60], which may also stimulate IL-6 production. Thus, it is

likely that in organoids fabricated with microvessels, there is more of a balance between inflammatory and non-inflammatory conditions, reflecting a more native-like adipose tissue. Consistent with this, TNF-α treatment downregulated adiponectin expression in only adipose organoids containing microvessels (figure 9(F)). TNF-α reduces the expression of adiponectin in non-diabetic, human adipose tissue [61]. It should also be considered, that, when normalizing adiponectin expression to GAPDH, the additional, non-adiponectin expressing cells brought in with microvessels may have slightly lowered the measured adiponectin levels. However, with even a generous estimate that 25% of the cells within the organoid could be vascular, there is still 1.5-fold decrease (log2) in adiponectin levels, which is a noteworthy difference. Clearly, more studies focusing on inflammation (acute and chronic) are needed to better evaluate the vascularized adipose organoid as a model of adipose tissue health and dysfunction.

5. Conclusion

We have developed a simple, robust, method for fabricating human vascularized adipose-like organoids. The fabrication approach used microvessels, isolated from adipose, as the source of the vascular elements within the organoids. Medium incompatibilities between adipocyte derivation and angiogenesis required us to develop a two-stage process in which cells are first committed to the adipocyte lineage and then combined with the isolated microvessels to build the organoid. Importantly, the fabrication process is amenable to a more high-throughput format in both the manufacture of the organoids and their use. Depending on additional matrix components included during fabrication, the organoids are likely useful in both research and therapeutic applications. Our findings indicate that the presence of the microvessels did not significantly alter adipocyte base function of lipolysis and adipokine expression with our protocol. However, the increased insulin receptor expression and altered responsiveness to an inflammation challenge indicate a more dynamic adipose tissue model. The general applicability of the fabrication process highlights the potential of the microvessel vascularization system for not only fabricating an *in vitro* adipose model, but other vascularized tissues as well.

Acknowledgments

The authors gratefully acknowledge Dr Matthew Weitzman for his assistance with confocal microscopy, Maddie Cook for her assistance with PCR, and Dr Kristen Johnson at the University of New Hampshire for use of her PCR equipment. Our funding sources are NSF 1842675 and NIH R01HL131856.

ORCID iDs

Hannah A Strobel https://orcid.org/0000-0002-2539-6529
James B Hoying https://orcid.org/0000-0001-7959-227X

References

[1] Dutta D, Heo I and Clevers H 2017 Disease modeling in stem cell-derived 3D organoid systems *Trends Mol. Med.* **23** 393–410
[2] Ranga A, Gjorevski N and Lutolf M P 2014 Drug discovery through stem cell-based organoid models *Adv. Drug Deliv. Rev.* **69–70** 19–28
[3] Skylar-Scott M A, Uzel S G M, Nam L L, Ahrens J H, Truby R L, Damaraju S and Lewis J A 2019 Biomanufacturing of organ-specific tissues with high cellular density and embedded vascular channels *Sci. Adv.* **5** 2459
[4] Spiller K L, Anfang R R, Spiller K J, Ng J, Nakazawa K R, Daulton J W and Vunjak-Novakovic G 2014 The role of macrophage phenotype in vascularization of tissue engineering scaffolds *Biomaterials* **35** 4477–88
[5] Gurevich D B, Severn C E, Twomey C, Greenhough A, Cash J, Toye A M, Mellor H and Martin P 2018 Live imaging of wound angiogenesis reveals macrophage orchestrated vessel sprouting and regression *EMBO J.* **37** 13
[6] Wise A F, Williams T M, Kiewiet M B G, Payne N L, Siatskas C, Samuel C S and Ricardo S D 2014 Human mesenchymal stem cells alter macrophage phenotype and promote regeneration via homing to the kidney following ischemia-reperfusion injury *Am. J. Physiol. Renal Physiol.* **306** F1222–35
[7] Roura S, Bagó J R, Soler-Botija C, Pujal J M, Gálvez-Montón C, Prat-Vidal C, Llucià-Valldeperas A, Blanco J and Bayes-Genis A 2012 Human umbilical cord blood-derived mesenchymal stem cells promote vascular growth *in vivo PLoS One* **7** e49447
[8] Hall C N, Reynell C, Gesslein B, Hamilton N B, Mishra A, Sutherland B A, O'Farrell F M, Buchan A M, Lauritzen M and Attwell D 2014 Capillary pericytes regulate cerebral blood flow in health and disease *Nature* **508** 55–60
[9] Alvino V V *et al* 2018 Transplantation of allogeneic pericytes improves myocardial vascularization and reduces interstitial fibrosis in a swine model of reperfused acute myocardial infarction *J. Am. Heart Assoc.* **7** 2
[10] Hoying J B, Utzinger U and Weiss J A 2014 Formation of microvascular networks: role of stromal interactions directing angiogenic growth *Microcirculation* **21** 278–89
[11] Strobel H A *et al* 2020 Stromal cells promote neovascular invasion across tissue interfaces *Front. Physiol.* **11** 1026
[12] Homan K A *et al* 2019 Flow-enhanced vascularization and maturation of kidney organoids *in vitro Nat. Methods* **16** 255–62
[13] De Moor L, Merovci I, Baetens S, Verstraeten J, Kowalska P, Krysko D V, De Vos W H and Declercq H 2018 High-throughput fabrication of vascularized spheroids for bioprinting *Biofabrication* **10** 035009
[14] Nashimoto Y, Okada R, Hanada S, Arima Y, Nishiyama K, Miura T and Yokokawa R 2020 Vascularized cancer on a chip: the effect of perfusion on growth and drug delivery of tumor spheroid *Biomaterials* **229** 119547
[15] Pham M T, Pollock K M, Rose M D, Cary W A, Stewart H R, Zhou P, Nolta J A and Waldau B 2018 Generation of human vascularized brain organoids *Neuroreport* **29** 588–93
[16] Wimmer R A *et al* 2019 Human blood vessel organoids as a model of diabetic vasculopathy *Nature* **565** 505–10
[17] Nunes S S, Greer K A, Stiening C M, Chen H Y S, Kidd K R, Schwartz M A, Sullivan C J, Rekapally H and Hoying J B 2010 Implanted microvessels progress through distinct neovascularization phenotypes *Microvasc. Res.* **79** 10–20

[18] Shepherd B R, Hoying J B and Williams S K 2007 Microvascular transplantation after acute myocardial infarction *Tissue Eng.* **13** 2871–9
[19] Shepherd B R, Chen H Y S, Smith C M, Gruionu G, Williams S K and Hoying J B 2004 Rapid perfusion and network remodeling in a microvascular construct after implantation *Arterioscler. Thromb. Vasc. Biol.* **24** 898–904
[20] Hoying J B, Boswell C A and Williams S K 1996 Angiogenic potential of microvessel fragments established in three-dimensional collagen gels *In Vitro Cell. Dev. Biol. Anim.* **32** 409–19
[21] Krishnan L, Hoying J B, Nguyen H, Song H and Weiss J A 2007 Interaction of angiogenic microvessels with the extracellular matrix *Am. J. Physiol. Heart Circ. Physiol.* **293** H3650–8
[22] Nunes S S, Rekapally H, Chang C C and Hoying J B 2011 Vessel arterial-venous plasticity in adult neovascularization *PLoS One* **6** e27332
[23] Utzinger U, Baggett B, Weiss J A, Hoying J B and Edgar L T 2015 Large-scale time series microscopy of neovessel growth during angiogenesis *Angiogenesis* **18** 219–32
[24] Nunes S S *et al* 2010 Angiogenic potential of microvessel fragments is independent of the tissue of origin and can be influenced by the cellular composition of the implants *Microcirculation* **17** 557–67
[25] Hiscox A M, Stone A L, Limesand S, Hoying J B and Williams S K 2008 An islet-stabilizing implant constructed using a preformed vasculature *Tissue Eng.* A **14** 433–40
[26] Gruionu G, Stone A L, Schwartz M A, Hoying J B and Williams S K 2010 Encapsulation of ePTFE in prevascularized collagen leads to peri-implant vascularization with reduced inflammation *J. Biomed. Mater. Res.* A **95** 811–8
[27] Weiss S *et al* 2010 Impact of growth factors and PTHrP on early and late chondrogenic differentiation of human mesenchymal stem cells *J. Cell. Physiol.* **223** 84–93
[28] Al-Nbaheen M, Vishnubalaji R, Ali D, Bouslimi A, Al-Jassir F, Megges M, Prigione A, Adjaye J, Kassem M and Aldahmash A 2013 Human stromal (mesenchymal) stem cells from bone marrow, adipose tissue and skin exhibit differences in molecular phenotype and differentiation potential *Stem Cell Rev. Rep.* **9** 32–43
[29] Wang C, Yin S, Cen L, Liu Q, Liu W, Cao Y and Cui L 2010 Differentiation of adipose-derived stem cells into contractile smooth muscle cells induced by transforming growth factor-β1 and bone morphogenetic protein-4 *Tissue Eng.* A **16** 1202–13
[30] Lee J H, Han Y S and Lee S H 2016 Long-duration three-dimensional spheroid culture promotes angiogenic activities of adipose-derived mesenchymal stem cells *Biomol. Ther.* **24** 260–7
[31] Bhang S H, Lee S, Shin J-Y, Lee T-J and Kim B-S 2012 Transplantation of cord blood mesenchymal stem cells as spheroids enhances vascularization *Tissue Eng.* A **18** 2138–47
[32] Larabee C M, Neely O C and Domingos A I 2020 Obesity: a neuroimmunometabolic perspective *Nat. Rev. Endocrinol.* **16** 30–43
[33] Francisco V, Pino J, Campos-Cabaleiro V, Ruiz-Fernández C, Mera A, Gonzalez-Gay M A, Gómez R and Gualillo O 2018 Obesity, fat mass and immune system: role for leptin *Front. Physiol.* **9** 640
[34] Klingelhutz A J, Gourronc F A, Chaly A, Wadkins D A, Burand A J, Markan K R, Idiga S O, Wu M, Potthoff M J and Ankrum J A 2018 Scaffold-free generation of uniform adipose spheroids for metabolism research and drug discovery *Sci. Rep.* **8** 523
[35] Daquinag A C, Souza G R and Kolonin M G 2013 Adipose tissue engineering in three-dimensional levitation tissue culture system based on magnetic nanoparticles *Tissue Eng.* C **19** 336–44
[36] Muller S *et al* 2019 Human adipose stromal-vascular fraction self-organizes to form vascularized adipose tissue in 3D cultures *Sci. Rep.* **9** 7250
[37] Turner P A, Gurumurthy B, Bailey J L, Elks C M and Janorkar A V 2017 Adipogenic differentiation of human adipose-derived stem cells grown as spheroids *Process Biochem.* **59** 312–20
[38] Zhang H and Zhang C 2009 Regulation of microvascular function by adipose tissue in obesity and type 2 diabetes: evidence of an adipose-vascular loop *Am. J. Biomed. Sci.* **1** 133
[39] Sibov T T *et al* 2012 Mesenchymal stem cells from umbilical cord blood: parameters for isolation, characterization and adipogenic differentiation *Cytotechnology* **64** 511–21
[40] Qian S-W, Li X, Zhang Y-Y, Huang H-Y, Liu Y, Sun X and Tang Q-Q 2010 Characterization of adipocyte differentiation from human mesenchymal stem cells in bone marrow *BMC Dev. Biol.* **10** 47
[41] Degawa-Yamauchi M, Moss K A, Bovenkerk J E, Shankar S S, Morrison C L, Lelliott C J, Vidal-Puig A, Jones R and Considine R V 2005 Regulation of adiponectin expression in human adipocytes: effects of adiposity, glucocorticoids, and tumor necrosis factor alpha *Obes. Res.* **13** 662–9
[42] Krogh-Madsen R, Plomgaard P, Keller P, Keller C and Pedersen B K 2004 Insulin stimulates interleukin-6 and tumor necrosis factor-alpha gene expression in human subcutaneous adipose tissue *Am. J. Physiol. Endocrinol. Metab.* **286** E234–8
[43] Cignarelli A, Genchi V, Perrini S, Natalicchio A, Laviola L and Giorgino F 2019 Insulin and insulin receptors in adipose tissue development *Int. J. Mol. Sci.* **20** 759
[44] Gregor M F and Hotamisligil G S 2011 Inflammatory mechanisms in obesity *Annu. Rev. Immunol.* **29** 415–45
[45] Abbott R D, Wang R Y, Reagan M R, Chen Y, Borowsky F E, Zieba A, Marra K G, Rubin J P, Ghobrial I M and Kaplan D L 2016 The use of silk as a scaffold for mature, sustainable unilocular adipose 3D tissue engineered systems *Adv. Healthcare Mater.* **5** 1667–77
[46] Lai N, Jayaraman A and Lee K 2009 Enhanced proliferation of human umbilical vein endothelial cells and differentiation of 3T3-L1 adipocytes in coculture *Tissue Eng.* A **15** 1053–61
[47] Aoki S, Toda S, Sakemi T and Sugihara H 2003 Coculture of endothelial cells and mature adipocytes actively promotes immature preadipocyte development *in vitro Cell Struct. Funct.* **28** 55–60
[48] Hammel J H and Bellas E 2020 Endothelial cell crosstalk improves browning but hinders white adipocyte maturation in 3D engineered adipose tissue *Integr. Biol.* **12** 81–89
[49] Li C Y, Wu X-Y, Tong J-B, Yang X-X, Zhao J-L, Zheng Q-F, Zhao G-B and Ma Z-J 2015 Comparative analysis of human mesenchymal stem cells from bone marrow and adipose tissue under xeno-free conditions for cell therapy *Stem Cell Res. Ther.* **6** 55
[50] Liu Y, Berendsen A D, Jia S, Lotinun S, Baron R, Ferrara N and Olsen B R 2012 Intracellular VEGF regulates the balance between osteoblast and adipocyte differentiation *J. Clin. Invest.* **122** 3101–13
[51] Bauman E, Feijão T, Carvalho D T O, Granja P L and Barrias C C 2018 Xeno-free pre-vascularized spheroids for therapeutic applications *Sci. Rep.* **8** 230
[52] Heiss M, Hellström M, Kalén M, May T, Weber H, Hecker M, Augustin H G and Korff T 2015 Endothelial cell spheroids as a versatile tool to study angiogenesis *in vitro Faseb J.* **29** 3076–84
[53] Fujimichi Y, Otsuka K, Tomita M and Iwasaki T 2019 An efficient intestinal organoid system of direct sorting to evaluate stem cell competition *in vitro Sci. Rep.* **9** 20297
[54] Acosta F M, Stojkova K, Brey E M and Rathbone C R 2020 A straightforward approach to engineer vascularized adipose tissue using microvascular fragments *Tissue Eng.* A **26** 1–10
[55] Charles B A, Doumatey A, Huang H, Zhou J, Chen G, Shriner D, Adeyemo A and Rotimi C N 2011 The roles of IL-6, IL-10, and IL-1RA in obesity and insulin resistance in African-Americans *J. Clin. Endocrinol. Metab.* **96** E2018–22

[56] Cawthorn W P and Sethi J K 2008 TNF-alpha and adipocyte biology *FEBS Lett.* **582** 117–31
[57] Han M S, White A, Perry R J, Camporez J-P, Hidalgo J, Shulman G I and Davis R J 2020 Regulation of adipose tissue inflammation by interleukin 6 *Proc. Natl Acad. Sci. USA* **117** 2751–60
[58] Tanaka T, Narazaki M and Kishimoto T 2014 IL-6 in inflammation, immunity, and disease *Cold Spring Harb. Perspect. Biol.* **6** a016295
[59] Wernstedt Asterholm I, Tao C, Morley T, Wang Q, Delgado-Lopez F, Wang Z and Scherer P 2014 Adipocyte inflammation is essential for healthy adipose tissue expansion and remodeling *Cell Metab.* **20** 103–18
[60] Zhang H H, Halbleib M, Ahmad F, Manganiello V C and Greenberg A S 2002 Tumor necrosis factor-alpha stimulates lipolysis in differentiated human adipocytes through activation of extracellular signal–related kinase and elevation of intracellular cAMP *Diabetes* **51** 2929–35
[61] Hector J, Schwarzloh B, Goehring J, Strate T, Hess U, Deuretzbacher G, Hansen-Algenstaedt N, Beil F-U and Algenstaedt P 2007 TNF-alpha alters visfatin and adiponectin levels in human fat *Horm. Metab. Res.* **39** 250–5